Water Vapour Climate Change Initiative (WV_cci) - CCI+ Phase 1

Product Validation and Intercomparison Report (PVIR) - Part 1: CDR-1 & CDR-2

Ref: D4.1

Date: 30 September 2021

Issue: 2.1

For: ESA / ECSAT

Ref: CCIWV.REP.016

This Page is Intentionally Blank

Project :	**Water Vapour Climate Change Initiative (WV_cci) - CCI+ Phase 1**
Document Title:	**Product Validation and Intercomparison Report (PVIR) - Part 1: CDR-1 & CDR-2**
Reference :	**D4.1**
Issued :	**30 September 2021**
Issue :	**2.1**
Client:	**ESA / ECSAT**

Author(s) : U. Falk (DWD), T. Trent (UoL), Rene Preusker (SE), Jürgen Fischer (SE), M. Schröder (DWD)

Document Change Log

Issue/ Revision	Date	Comment
0.9	28 July 2020	Initial issue submitted to project coordination for review
1.0	31 July 2020	First issue for submission to ESA
1.1_draft	14 Sep 2020	Feedback from co-authors to RID's implemented
1.1	13 October 2020	RID's from ESA implemented
1.2	21 May 2021	Correction to equation 4.8
2.0	21 August 2021	Version submitted to ESA prior to AR3
2.1	30 September 2021	Feedback from AR3 implemented, RIDs from ESA answered

TABLE OF CONTENTS

INDEX OF TABLES

INDEX OF FIGURES

1. INTRODUCTION

1.1 Purpose

This document is the Product Validation and Intercomparison Report (PVIR) for the ESA Water Vapour Climate Change Initiative project (WV_cci) Part 1. It contains the validation and intercomparison results for CDR-1 and CDR-2, i.e. the atmospheric total column water vapour (TCWV) data records produced by WV_cci. The PVIR utilises CDR-1 and CDR-2 in version 3.1 which covers the period July 2002 and December 2017. Ground-based, *in situ*, and satellite-based as well as reanalysis (ERA5) data records are used as reference and for comparison and are compared to the WV_cci data records as described in detail in the Product Validation Plan (PVP v3.2).

This PVIR document is split into two parts:

- Part 1 contains the validation and intercomparison of CDR-1 and CDR-2,
- Part 2 contains the validation and intercomparison of CDR-3 and CDR-4.

This document is PVIR Part 1.

1.2 Scope

The scope of the product validation and intercomparison efforts within the ESA WV_cci project is to assess and validate TCWV datasets as well as attached uncertainties of each product, in order to prepare datasets for the climate research community. By exploiting synergies between microwave and NIR sensors in Earth Observation missions, time series of global coverage TCWV are produced. The evaluation of TCWV and uncertainties derived from NIR sensors for land surfaces (CDR-1) is assessed prior to the assessment of the combined product of microwave and NIR TCWV data (CDR-2). Finally, the compliance with requirements is tested.

1.3 The ESA Water_Vapour_cci project

Water vapour is the single most important natural greenhouse gas in the atmosphere, thereby constraining the Earth's energy balance, and it is also a key component of the water cycle. Due to its importance, the WMO's Global Climate Observing System (GCOS) program has highlighted water vapour as an Essential Climate Variable (ECV) in the GCOS 2016 Implementation Plan. There is consequently the need to consolidate our knowledge

of natural variability and past changes in water vapour and to establish climate data records of both total column and vertically resolved water vapour for use in climate research. These climate data records need to be homogeneous in space and time, which bears great challenges due to changing instrument characteristics and performances. Well-characterised uncertainties are a key attribute of such climate data records in order to reduce the uncertainty in estimates of climate change and global radiative forcing.

The Climate Change Initiative (CCI) is a program of the European Space Agency (ESA), established to tackle the challenges encountered in merging climate data records of ECVs and has the goal to provide climate modellers and researchers with long-term satellite records from current and past European (and other space agencies') missions. The ESA CCI Water Vapour project generates stratospheric and tropospheric water vapour by developing novel methods to determine, merge and estimate such water vapour data and associated uncertainties.

1.4 WV_cci datasets

The WV_cci datasets comprise four CDRs that are compared with and validated by ground-based, *in situ*, airborne and satellite-based data records as described in detail by the Product Validation Plan (PVP v3.2):

- CDR-1: gridded monthly and daily time series of TCWV in units of kg/m^2 that cover the global land areas with a spatial resolution of 0.05° and 0.5°. It covers the period July 2002 to December 2017, and is a combined product of MERIS, MODIS and HOAPS.
- CDR-2: gridded monthly and daily time series of TCWV in units of kg/m^2 that cover the global land and ocean areas with a spatial resolution of 0.05° and 0.5°. It covers the period July 2002 to December 2017, and combines WV_cci CDR-1 with CM SAF HOAPS (microwave imager based) data records.
- CDR-3 contains the vertically resolved water vapour ECV in units of ppmv (volume mixing ratio) and is provided as zonal monthly means on the SPARC Data Initiative latitude/pressure level grid (SPARC, 2017; Hegglin et al., 2013). It covers the vertical range between 250 hPa and 1 hPa, and the time period 1985 to the end of 2019.
- CDR-4 consists of three-dimensional vertically resolved monthly mean water vapour data (in ppmv) with spatial resolution of 100 km, covering the troposphere and lower stratosphere.

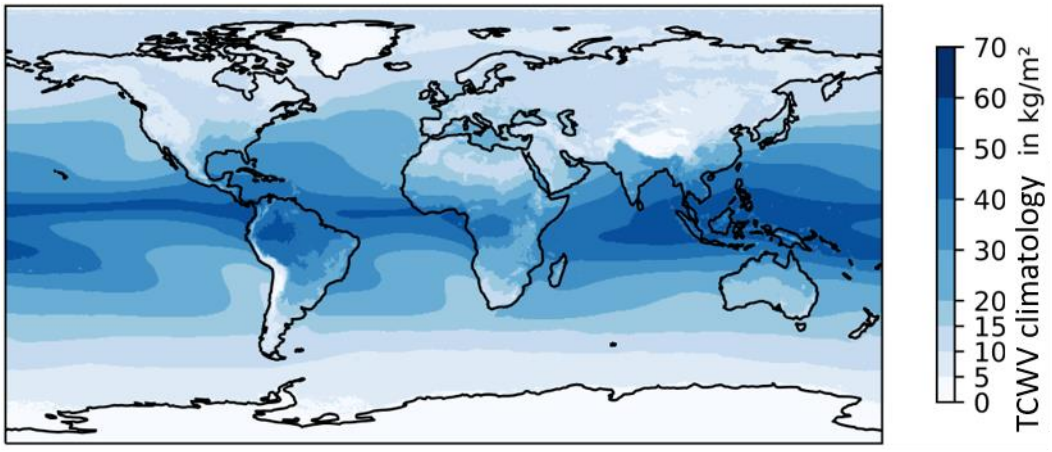

Figure 1-1: Global map of TCWV climatology of the WV_cci CDR-2 (version fv3.1) over the time period July 2002 to December 2017.

Figure 1-1 shows the TCWV climatology of the WV_cci CDR version fv3.1 over the time period July 2002 to December 2017.

2. VALIDATION STRATEGY

2.1 Datasets

An extensive evaluation of TCWV data products and their attached uncertainties has been carried out based on reference data sets and intercomparison data sets as outlined in the Product Validation Plan (PVP v3.2).

Round robin efforts focused on the validation of Level 2 TCWV data over land using SuomiNet data as reference. Associated results are discussed in section 3.

The remaining part of the PVIR focuses on the validation of the final, gridded Level 3 products from WV_cci, TCWV over land surfaces (CDR-1) and over land and ocean surfaces, i.e. globally (CDR-2) are considered. The validation is, thus, subdivided into subsections accordingly.

The validation was carried out against the reference and comparison data records:

1. Merged Microwave by REMSS (MMW), ERA5, AIRS (including AMSU) version 6 (AIRS), the predecessor version to the WV_cci TCWV CDR-2 by C3S (C3S), GOME Evolution (GOME) and IMS for the spatial assessment of biases and cRMSD.

2. ERA5, AIRS, C3S, SuomiNet and GRUAN for global land surfaces.

3. MMW, AIRS, ERA5, C3S, GOME and IMS for global coverage and global ice-free ocean surfaces.

All datasets used for validation and intercomparison are referenced and described in the Data Access Requirement Document (DARD, v3.2).

2.2 Methodology

The WV_cci data products of TCWV are validated against reference datasets declared in the DARD (v3.2). The methodology and metric underlying this Product Validation and Intercomparison Report (PVIR) is defined in the Product Validation Plan (PVP, v3.2).

The evaluation is divided into the following tasks:

1. Validation of NIR Level 2 data records against *in situ* observations from SuomiNet and MWR data.
2. Spatial comparison between CDR and comparison data records.
3. Comparison of time series between CDR and reference as well as comparison data records.
    a. CDR-1, i.e. global land surfaces.
    b. CDR-2, i.e. global and global ice-free ocean surfaces.
    c. CDR-2, i.e. global ice-free ocean and land surfaces, i.e., excluding sea ice and coastal areas.
4. Analysis of homogeneity and stability.
5. Assessment of consistency.
6. Compliance with product and user requirements.

A summary of validation statistics is given in Table 5-1, Table 5-2 and Table 7-1.

3. VALIDATION OF NIR LEVEL 2 DATA

The quantification of uncertainties based on comparisons with ground-based measurements are demonstrated with MERIS; MODIS and OLCI Level 2 results of the WV_cci TCWV algorithm that were used as input for CDR vf3.1.

For the validation of the TCWV products, estimated from MERIS and MODIS measurements within the timeframe 2002 to 2011, we used the ARM microwave based TCWV retrievals, because of the high accuracy of this product. Only MERIS and MODIS measurements are taken which are cloud-free in an area of about 10 x 10 km^2 around the ARM stations. For the cloud detection, the standard L2 cloud-mask has been applied (including the cloud ambiguous and cloud margin flags). Due to the strict requirements for the comparisons between satellite and ground-based measurements the number of cases is quite limited. The comparison of MERIS and MODIS and ARM TCWV retrievals show a very high agreement, no wet- or dry bias is found as detected in the TCWV standard product. The correlation between both quantities is 0.98, while MERIS has a root-mean-squared-difference of 1.8 kg/m^2 and MODIS Terra has a RMSD of 1.3 kg/m^2 (see Figure 3-1 and Figure 3-2).

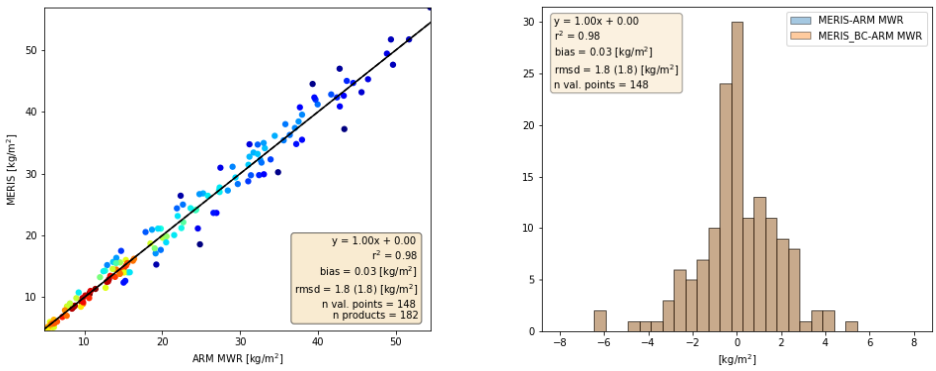

Figure 3-1: Comparison between MERIS and ARM-microwave based TCWV retrievals.

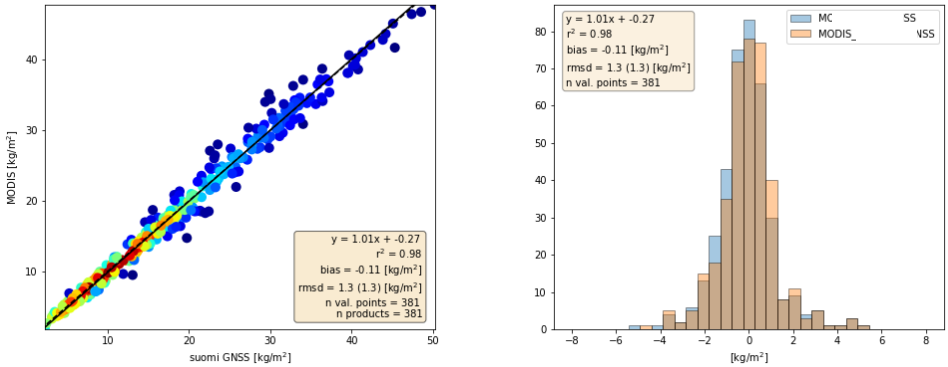

Figure 3-2: Comparison between MODIS and ARM-microwave based TCWV retrievals.

OLCI A/B measurements are taken for the validation above land surfaces, if they are cloud-free in an area of about 10 x 10 km^2 around the GNSS stations. For the cloud detection, the standard OLCI L2 cloud-mask has been applied (including the cloud ambiguous and cloud margin flags). Nearly 3000 matchups within the period between August 2018 and January 2019 have been analysed. The scenes cover high and low elevations, however, the majority of the used SuomiNet ground stations are located in North and Central America. The comparison of OLCI and GNSS based TCWV retrievals shows a very high agreement. The correlation between both quantities is 0.98. The root-mean-squared-difference is 1.3 kg/m^2. There is nearly no systematic overestimation contrary to 13% by OLCI as found for the standard ground-processor before. The bias corrected *RMSD (cRMSD)* is only 1.2 kg/m^2 (see Figure 3-3).

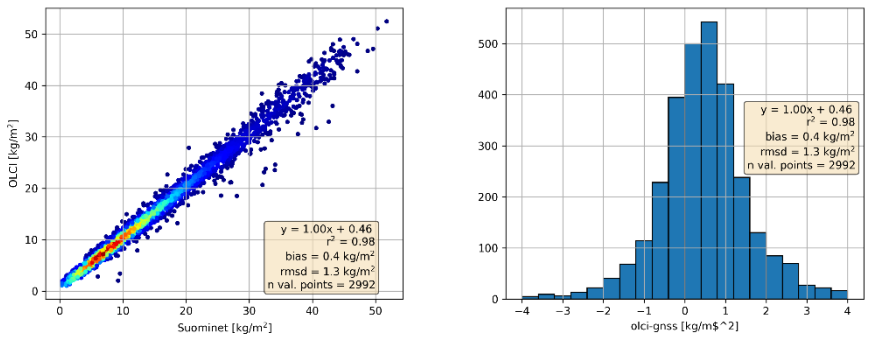

Figure 3-3: Comparison between OLCI and GNSS based TCWV.

4. VALIDATION AND INTERCOMPARISON OF WV_CCI PRODUCTS

This section presents the WV_cci validation results for the TCWV products CDR-1 and CDR-2 produced within the project's framework. The latest and final version of CDR-1 and CDR-2 is version 3.1. The version is based on latest developments within the project. Validation efforts were carried out taking all valid collocations with TCWV > 0 kg m^{-2} of CDR with reference dataset into account.

Average statistics are provided in Table 5-2 and Table 7-1 in sections 5 and 7. Results from homogeneity and stability analysis are given in section 5.

4.1 Spatial assessment of bias and cRMSD with global coverage

The coverage of CDR-2 encompasses global land and ocean surfaces, as well as coastal and sea-ice areas. The surface type flag incorporated into CDR-2 differentiates between land, ocean, sea-ice regions, coastal areas, different amount of cloud coverage over land and regions with heavy precipitation over ocean. This allows for a distinct revision of statistical measures according to the respective surface types. Note that CDR-1 is included in CDR-2, i.e. CDR-1 and CDR-2 land are identical.

The spatial distribution of bias and cRMSD between CDR-2 against the different intercomparison and reference datasets is shown in Figure 4-1. The Merged Microwave data records (REMSS) are only available over global ice-free ocean, thus, large parts are white. Distinct spatial patterns are evident over the ITCZ, storm track regions and rain forests. The spatial bias assessment shows a pattern of slightly dry and slightly wet biases that roughly follows the global cloud pattern. A wet (positive) bias means that the CDR contains more water vapour than the reference data. It is depicted in blue. A dry (negative) bias is shown in red, and refers to a dry bias, meaning the CDR contains less water vapour for the respective data points. Over land the bias is generally negative while it is generally positive over ocean, except for the comparison to the Merged Microwave dataset. The cRMSD has its maximum at the ITCZ and exhibits a land / sea contrast. Largest absolute biases are observed over ocean relative to IMS and largest cRMSD is observed over the ITCZ and storm tracks relative to GOME Evolution. The bias is generally small relative to Merged Microwave and C3S. The cRMSD is smallest relative to Merged Microwave, C3S and AIRS, and for GOME and IMS generally higher. The intercomparison shows a distinct bias (ERA5, GOME) and cRMSD (ERA5, AIRS, GOME) over sea-ice regions.

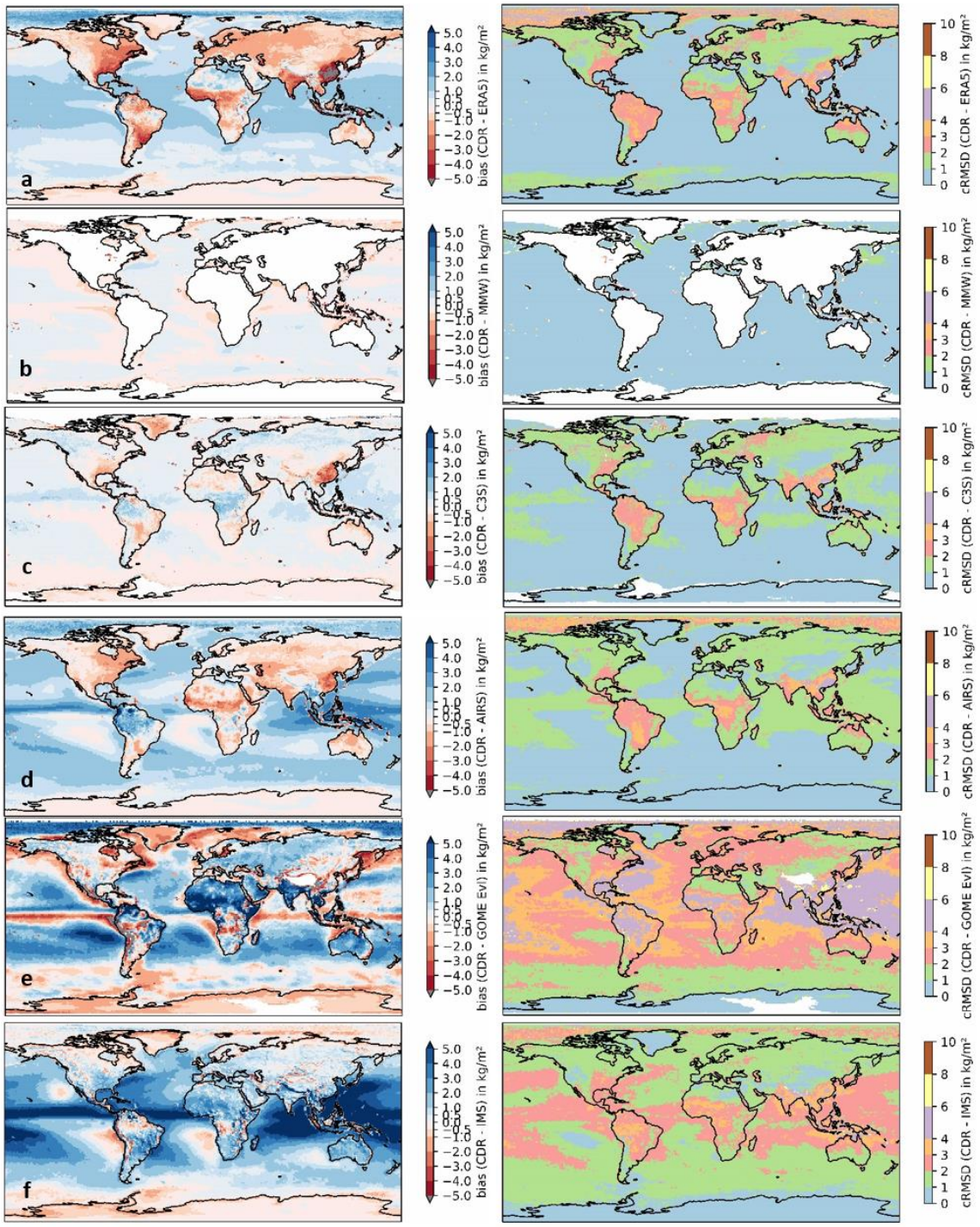

Figure 4-1: Spatial maps of bias (left) and cRMSD (right) of CDR-2 against reference and intercomparison datasets: (a) ERA5, (b) Merged Microwave (MMW), (c) C3S precursor to WV_cci CDR-2, (d) AIRS with AMSU version 6, (e) GOME Evolution and (f) IMS. Missing data is indicated in white in the cRMSD maps.

It became apparent that inland water bodies exhibit opposite signs in bias depending on the predominant sensor of the time period. Thus, associated data needs to be handled with care. Therefore, a global map of water bodies (inland and global ocean) by the ESA CCI LandCover project was resampled from the original spatial resolution of 150 m to the here relevant spatial resolution of 0.5° and 0.05°. The mask is available as auxiliary data.

Figure 4-2: Mask of water bodies (oceans and inland open water surfaces) as resampled from 150 m-resolution map provided by the LandCover CCI, © ESA Climate Change Initiative - Land Cover led by UCLouvain (2017).

4.2 Validation over global land surfaces (CDR-1)

The validation of the final level 3 (L3) data record (CDR-1 fv3.1) was carried out against data records from the global observation networks GRUAN and SuomiNet. The CDR-1 product is also compared to ERA5, AIRS, ARSA and C3S data records for global land surfaces.

The GRUAN dataset consists of radiosonde observations measuring the profiles of atmospheric variables, that allow for the calculation of TCWV. The spatial coverage of this network can be considered rather low. Analysis of valid collocations between the radiosonde observation sites and the CDR-1 gridded data show a low amount of collocations per day and even month. The respective statistical measures of daily and monthly bias and cRMSD cannot be considered meaningful. Thus, only a scatter plot of associated results is shown.

The SuomiNet network consists of globally distributed permanent stations of GPS receivers conducting real-time atmospheric precipitable water vapour measurements. The number of stations is substantially higher than in the GRUAN dataset.

Note that time series per station are frequently affected by data gaps (see Figure A3-0-1). Such variability might hamper the interpretation of results.

Figure 4-3 shows the time series of bias and cRMSD relative to reference and comparison datasets over global land surfaces. The bias and cRMSD are generally small and within ±1.5 kg/m^2 and 2.5 kg/m^2, respectively. Bias and cRMSD exhibit increased absolute values at the early part of the considered period for unknown reasons and at the end of period when OLCI data enters in April 2016. Also notable is a change in bias and cRMSD when MODIS data enters the product. Overall, the bias is close to 0 kg/m^2, except for a negative bias relative to ERA5. The cRMSD exhibits values around 2 kg/m^2, except relative to C3S where it is smaller. Results for SuomiNet are affected by a large variability. The cRMSD exhibits a change in early 2003 and when OLCI data enters CDR-2. Also, the temporal variability of cRMSD of the MODIS period differs from the rest of the time series. The latter might be caused by differences in cloud masking between MODIS and MERIS/OLCI (see below).

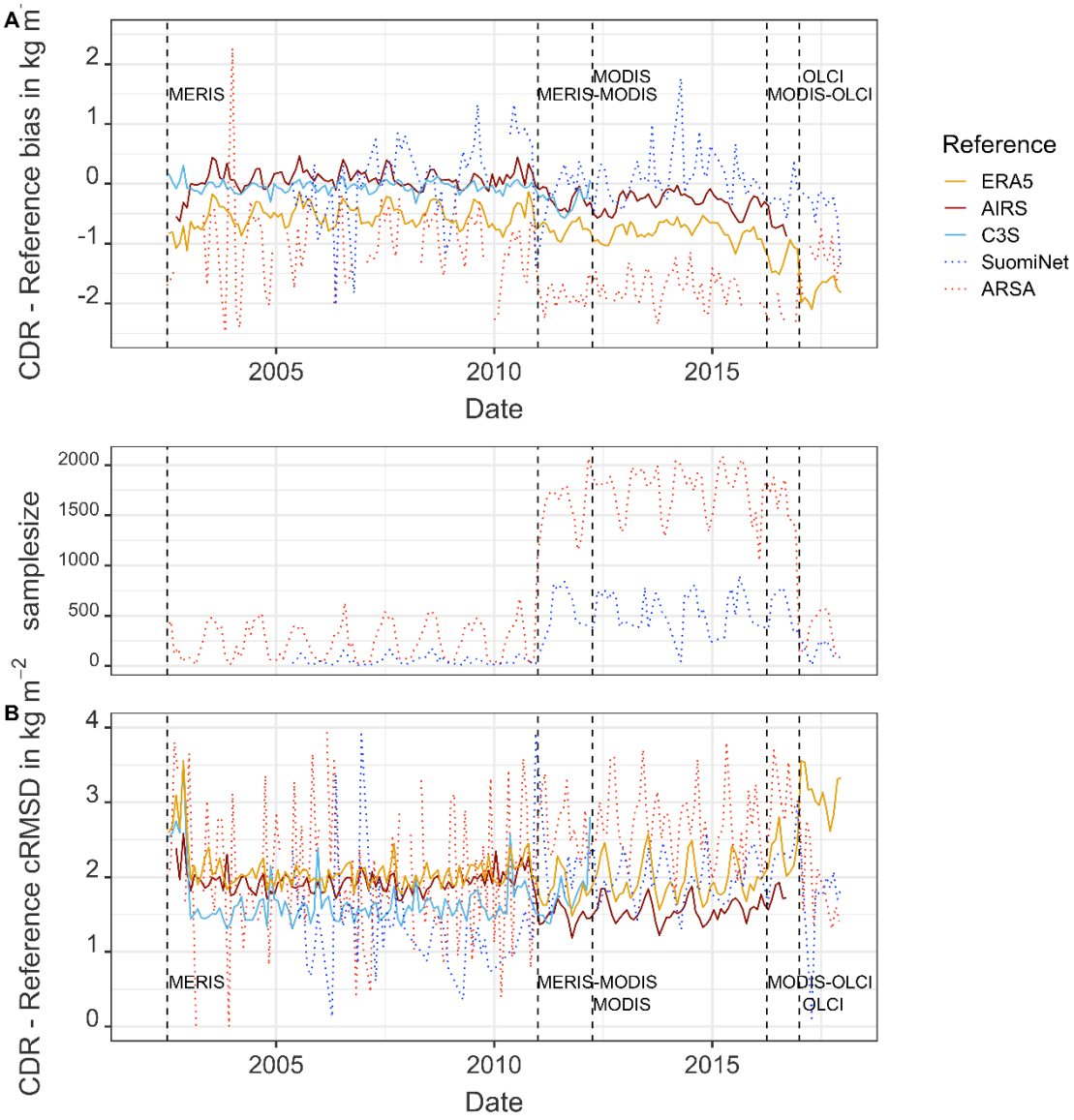

Figure 4-3: Time series of (A) bias and (B) cRMSD between CDR-1 and the intercomparison and reference dataset for global land surfaces. The dashed vertical lines mark changes in the NIR observing system. The sample size contains the number of valid daily observations in a month (middle panel).

When looking at missing data in MERIS, MODIS and OLCI periods it became obvious that the MODIS cloud mask is less strict than the cloud masks for MERIS and OLCI (not shown). This also means that in particular in the northern extra-tropics significantly more valid values are present in the MODIS than in the MERIS and OLCI data. When computing (near) global spatial averages this will cause a discontinuity when MODIS data enters and leaves the data record. Thus, a common mask should be applied for homogeneity reasons when

global averages are used in climate change analysis context. This mask, derived to identify grid points that have valid TCWV values for all time steps over the time period July 2002 to March 2016, was generated within WV_cci and is shown in Figure 4-4. The mask is available as auxiliary data.

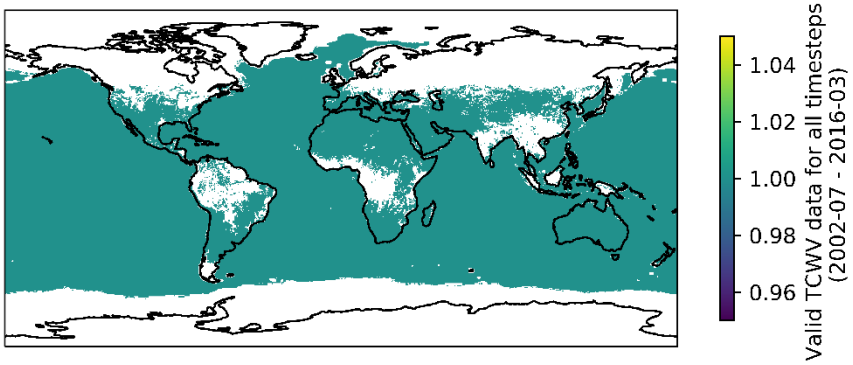

Figure 4-4: Mask of valid TCWV values in CDR-2 over all time steps In time period July 2002 to March 2016.

A change in bias is observed when MODIS data enter the product (see Figure 4-3). Given the results from the clear-sky bias analysis (CAR v3.0) this bias in combination with a change in cloud mask might explain the observed changes in bias. In order to compare like-to-like CDR-1 and ERA5, the ERA5 data is sampled such that only clear-sky values at 10:00 local time are used. At the same time grids from CDR-1 are only considered when all values are within 0.25°, the spatial resolution of ERA5, are valid, i.e. clear-sky.

Figure 4-5 shows the time series of bias and cRMSD of associated results. First of all it shows a systematic difference between the bias relative to ERA5 daily and ERA5 monthly. This bias is likely dominated by the clear-sky bias and is indeed in the same order as the average clear-sky bias of approximately -0.9 kg/m^2 (CAR v3.0). This is supported by the fact that the surface type flag indicates partly cloudy cases over more or less all land surfaces in monthly files. When looking at daily values the difference is in the subgrid sampling, i.e. within 0.25°. Here differences in cloud masking and associated differences in sampling the clear-sky bias seemingly cause a small change in bias between MERIS and MODIS. However, this effect does not explain the increase in absolute bias when OLCI becomes available.

It might be argued that the spatial variability of the bias (Figure 4-1) in combination with differences in the cloud mask might also explain the observed features. However, when

constructing the clear-sky ERA5 and CDR-1 data, differences in spatial sampling are still present if not enhanced.

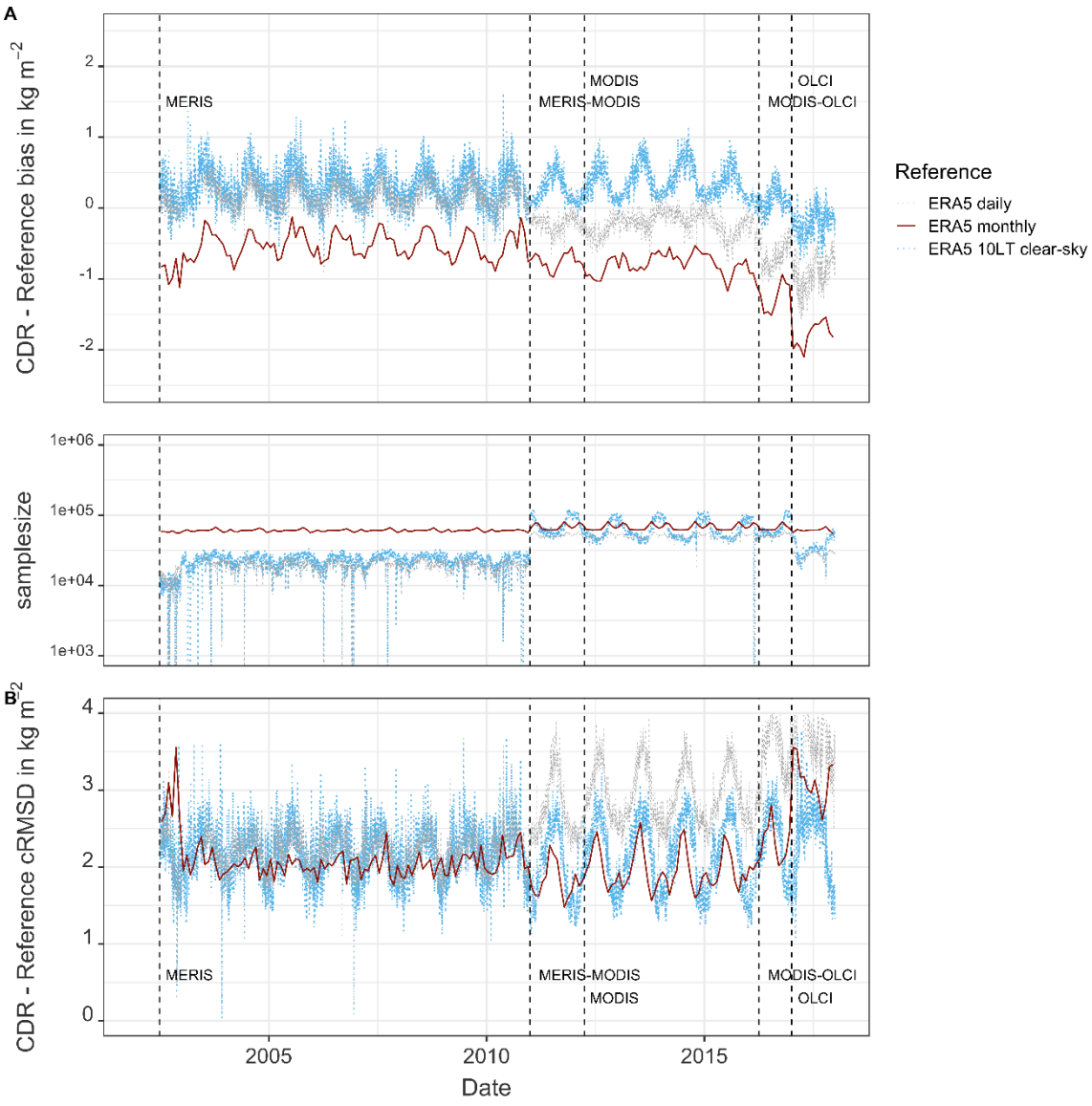

Figure 4-5: Time series of (A) bias and (B) cRMSD between CDR-1 and ERA5 for monthly and daily temporal resolution and ERA5 with clear-sky filter and 10 LT (local time) sampling time for global land surfaces. The dashed vertical lines mark changes in the NIR observing system. The middle panel shows the number of valid collocations.

Scatter plots between CDR-1 and SuomiNet as well as GRUAN are shown in Figure 4-6 and Figure 4-7, respectively. In both cases valid collocations are close to the 1-by-1 line and exhibit a good degree of correlation. Also in both cases a few outliers are present at values between 25 and 60 kg/m^2, with CDR-1 having typicallylarger values than the reference.

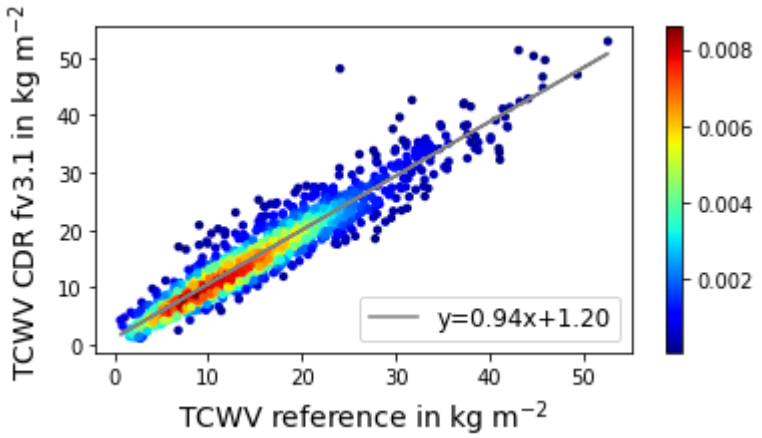

Figure 4-6: Scatter plot of daily TCWV (CDR-1) against the reference dataset SuomiNet for global land surfaces. The linear regression yields R^2 = 0.94. The colour map shows the density of data points.

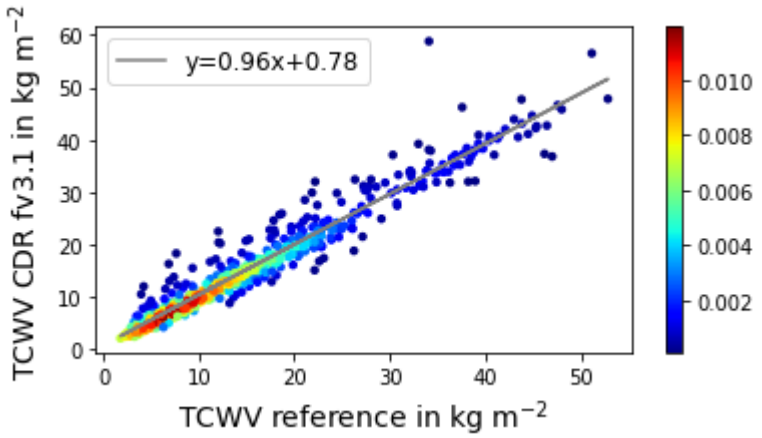

Figure 4-7: Scatter plot of daily TCWV (CDR-1) against the reference dataset GRUAN. The linear regression yields R^2 = 0.94. The colour map shows the density of data points.

4.3 Validation of the global product (CDR-2) and for global ice-free ocean

The validation of the final level 3 (L3) data record (CDR-2 fv3.1) is carried out separately for global ice-free ocean and global surfaces. The comparisons were carried out against Merged Microwave, AIRS, C3S and ERA5 over global ice-free oceans and against AIRS, C3S, and ERA5 over global surfaces (see PVP, v3.2). The comparison of TCWV from CDR-2 over ice-free ocean to the various data records is essentially a validation of the CM SAF HOAPS data in CDR-2. The Merged Microwave data records includes data from 11 satellite-borne microwave imaging radiometers merged into a gridded monthly time series (Mears et al. 2018). More details are given in the DARD v3.2 and the PVP v3.2.

Figure 4-8 shows the time series of bias and cRMSD relative to reference and comparison datasets over global ice-free oceans. The bias results are separated into two levels: one level close to 0.0 kg/m^2 relative to Merged Microwave and C3S and one close to 0.75 kg/m^2 relative to AIRS and ERA5. The comparison to C3S exhibits partly an annual cycle in bias. The cRMSD is around 0.8 kg/m^2, except for the comparison to AIRS where the level is at 1.1 kg/m^2. The cRMSD relative to C3S exhibits a biannual cycle for unknown reasons while the peaks in cRMSD relative to AIRS are not present in the other comparisons and thus likely an AIRS issue. Else, the cRMSD exhibits a fairly constant behaviour in time.

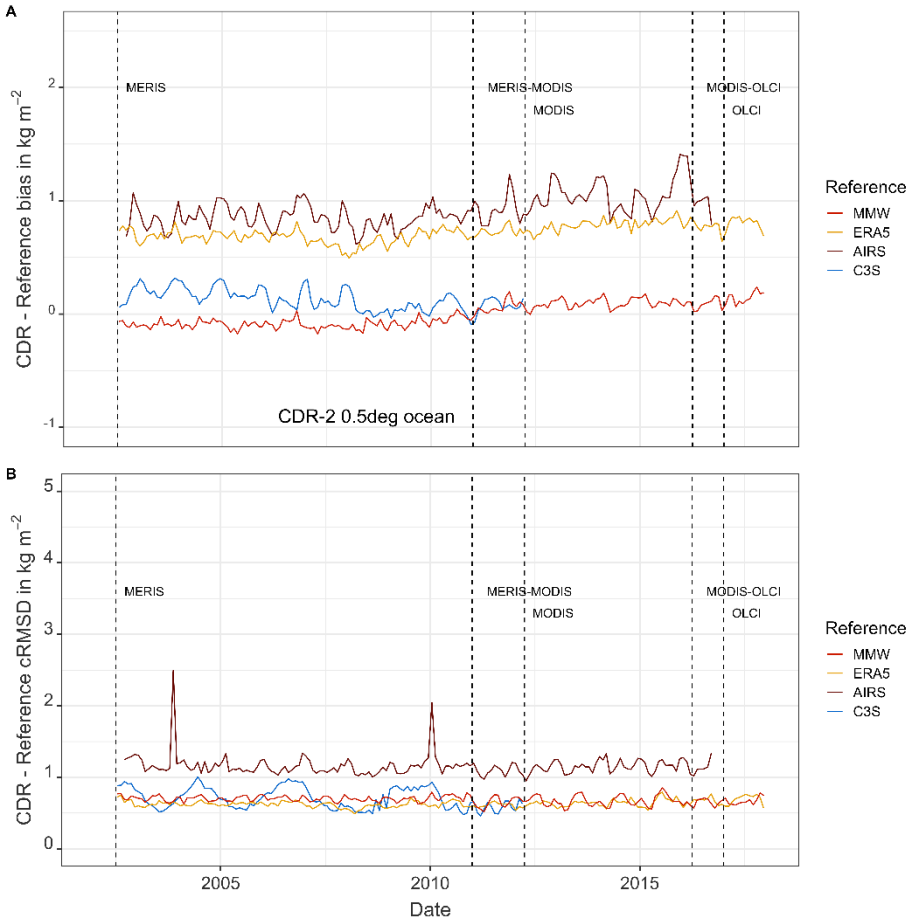

Figure 4-8: Time series of (A) bias and (B) cRMSD between CDR-2 and the intercomparison and reference datasets for global ice-free ocean surfaces. Note that only microwave-based HOAPS data are utilised here. The vertical lines indicating changes in the NIR input are kept for consistency.

Figure 4-9 shows the time series of bias and cRMSD relative to reference and comparison datasets over global surfaces. The results for the bias are again separated into two levels: close to 0.0 kg/m^2 relative to ERA5 and C3S and 0.6 kg/m^2 relative to AIRS and GOME Evolution. Obviously, the positive and negative biases over ocean and land for ERA5, respectively, compensate each other. The cRMSD exhibits values around 1.5 kg/m2, except for GOME Evolution where the level is at 3.5 kg/m^2. Peaks present in the cRMSD relative to AIRS are again likely an AIRS issue. The cRMSD exhibits a small change in early 2003 and when OLCI data enters CDR-2. Also, the temporal variability of cRMSD of the MODIS period differs from the rest of the time series. The latter might be caused by differences in cloud masking between MODIS and MERIS/OLCI.

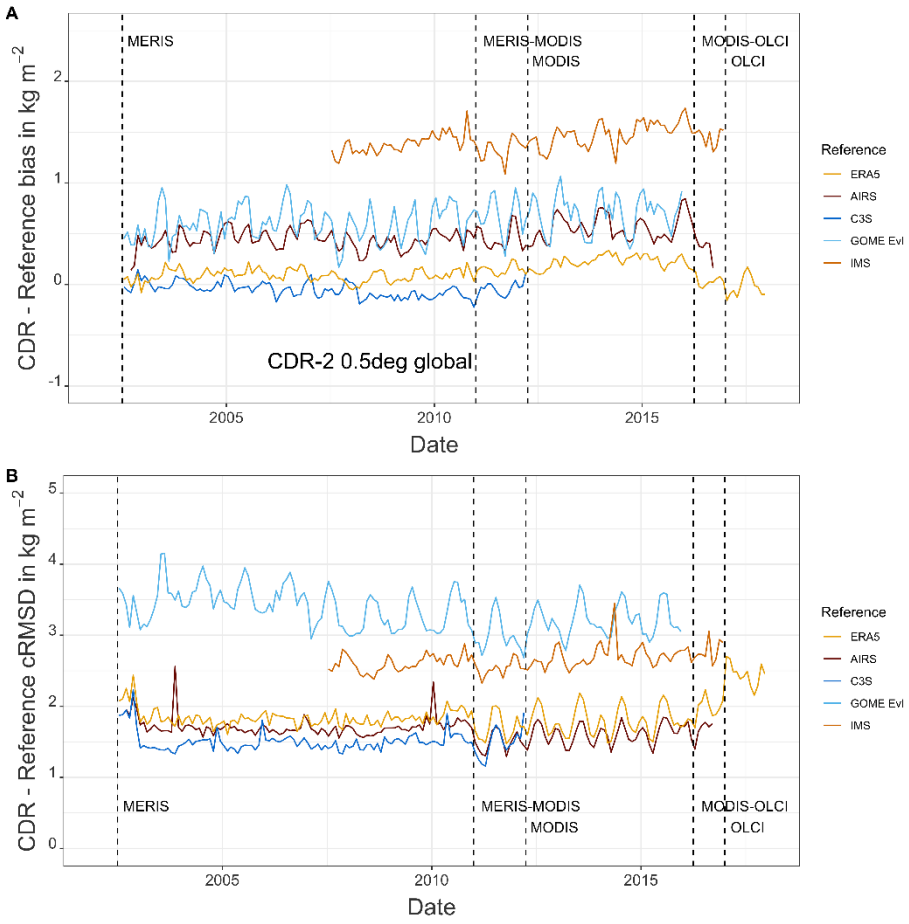

Figure 4-9: Time series of (A) bias and (B) cRMSD between CDR-2 and the intercomparison and reference dataset for global (all) surfaces.

As mentioned in section 4.2 inland water bodies are affected by increased uncertainties. Also, the retrieval over coastal areas has reduced quality as the need for sufficiently large reflected radiation is not valid usually (ATBD Part 1, v2.1). Figure 4-10 shows an anomaly times series for TCWV data over sea-ice and coasts, and for inland water bodies, sea-ice and coasts. Though the anomaly is small it exhibits an increase in anomaly when MODIS data enters CDR-2.

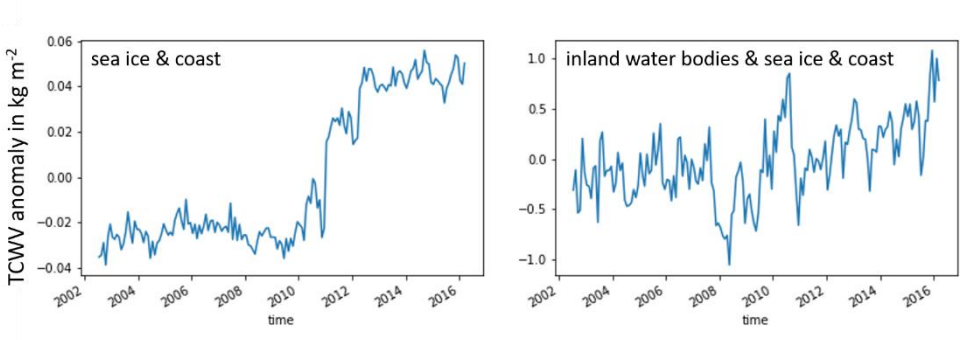

Figure 4-10: Anomaly time series of WV_cci CDR-2 TCWV for surface types (left) sea ice and coast and (right) sea ice, coast and inland water bodies. Please note that the left and right y-axes have different scales.

Thus, also time series of bias and cRMSD are analysed over global land and ocean surfaces, i.e. excluding sea-ice, coasts and inland water bodies. Associated results are shown in Figure 4-11 for the same reference and comparison data records as for the global comparison. Relative to the global results, the bias is generally slightly larger. The MODIS period instead seems to be at a slightly lower level such that the bias seems to be slightly more stable. The cRMSD is generally smaller (only marginal for GOME Evolution).

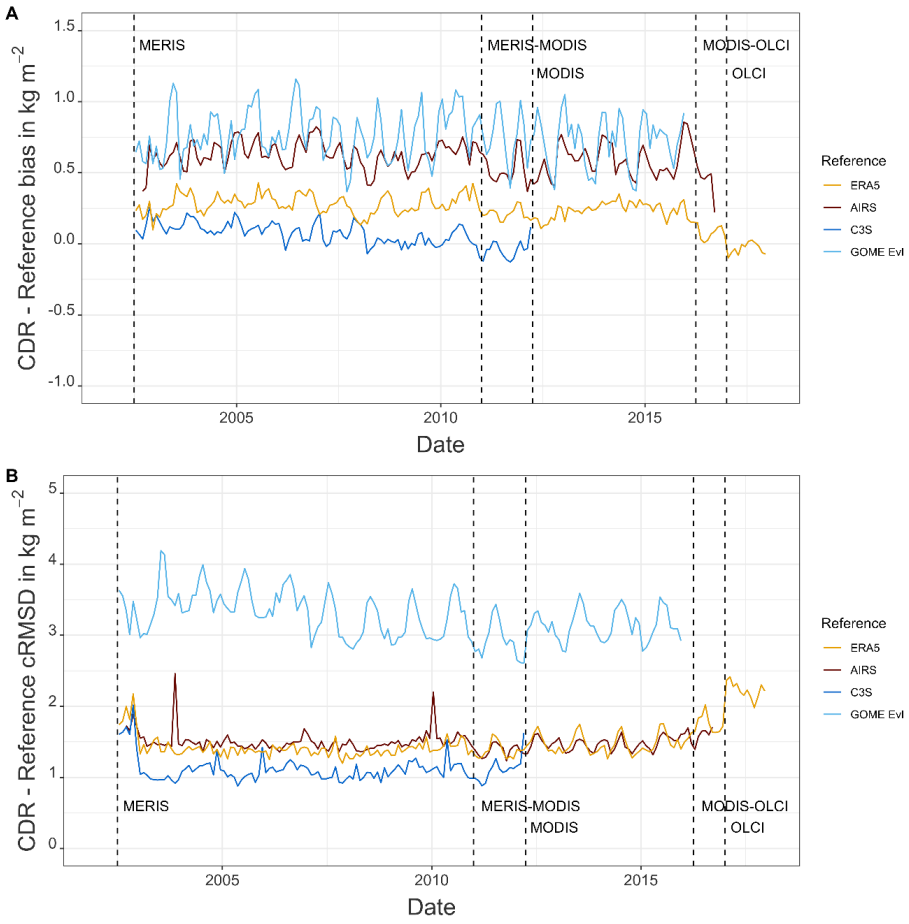

Figure 4-11: Time series of bias and cRMSD between CDR-2 and the intercomparison and reference dataset for global land and ocean surfaces (no coast, sea ice, inland water bodies).

Finally, Figure 4-12 shows scatter plots between CDR-2 and Merged Microwave over the global ice-free ocean and between CDR-2 and AIRS over global surfaces. Both plots exhibit a high level of correlation ($R^2 \geq 0.99$) with the bulk of the data pairs being close to the one-to-one line. In the global comparison the spread is a bit wider and a few outliers are observed at small CDR-2 TCWV values. To some extent this can be explained with a reduced quality of CDR-2 over sea-ice and coasts.

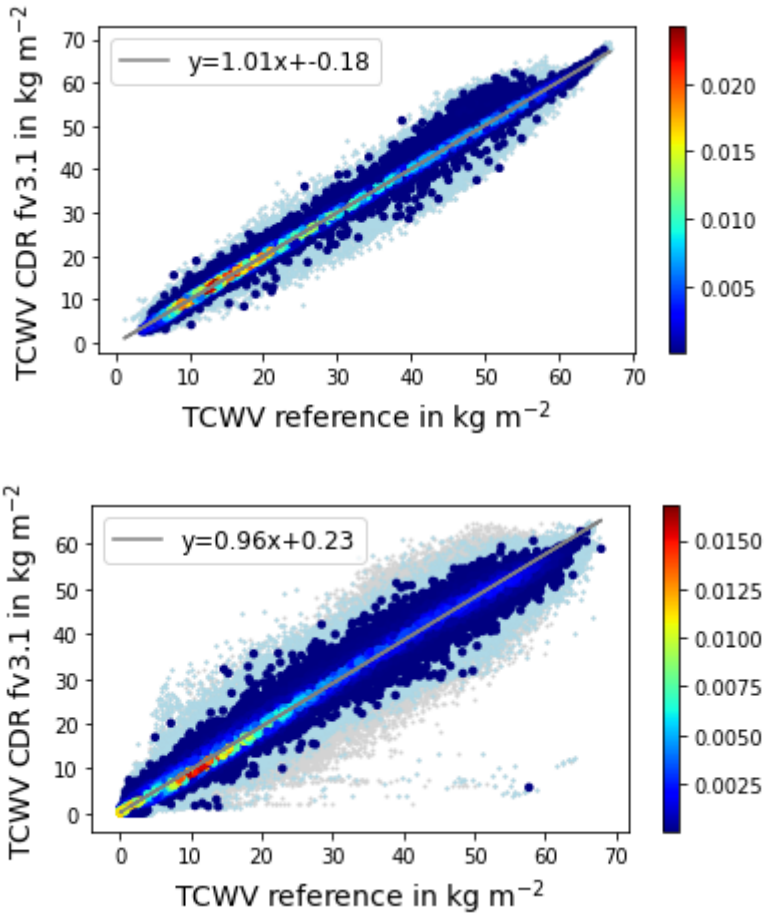

Figure 4-12: Scatter plots of daily TCWV (CDR-2 fv3.1) against TCWV of Merged Microwave (top) and AIRS (bottom) for ice-free ocean and global surfaces, respectively. The linear regression yields R^2 = 1.0 for Merged Microwave and R^2 = 0.99 for AIRS. Due to the large amount of collocations, 100,000 data points were chosen randomly to provide density colour scale. Other data points are light blue. Data points that are associated with surface types "coast" and "sea ice" are depicted in grey.

5. HOMOGENEITY AND STABILITY ANALYSIS

The assessment of homogeneity in CDR-1 and CDR-2 includes analysis of results from the Penalised Maximal F (PMF, Wang, 2008a, b) and the Standard Normal Homogeneity (SNH, Reeves et al., 2007) tests. Input to the tests are anomaly differences, i.e. the annual cycle has been removed from CDR and comparison data set and then the difference between both anomalies is used as input to the tests. Results contain information on potential break points in the anomaly difference time series. Associated information includes the time of the break point and its step size or strength. Details and cautionary notes are given in Schröder et al. (2016, 2019). It is recalled that the uncertainty is in the order of ±3 months and it is possible that break points are missed. The results of the homogeneity test are summarised in Table 5-1. In addition, the break points are also marked as vertical lines in the stability plots (Figure 5-1 – Figure 5-3). In case the date of the break point coincides with known changes in the observing system or changes of the retrieval system it is mentioned in the event column. For TCWV over land, ocean and global break points are observed. Only two break points are confirmed by the double test: one over land and one over ocean. The break point observed in the global time series coincides with the break point over land which itself coincides with the inclusion of OLCI data. Note that this change in behaviour is also evident in the time series of cRMSD (Figure 4-3). Between July 2006 and March 2010 the SSMIS sensors became operational while three SSM/I sensors stopped operation or were removed due to a radar calibration beacon (see e.g. Schröder et al., 2016). Though the break points at 2009-12 and 2006-11 coincide with changes in the observing system this period also seems to exhibit a general increase in bias. Note that the step size and the overall noise level is very small (see Figure 5-2).

Table 5-1: Results from homogeneity test. Break points are marked green if the PMF test is confirmed by the SNH test

CDR-1 & CDR-2 surface type	Ref. dataset	Break point (yyyy-mm)	Step size (kg/m^2)	Event
Land	AIRS	n/a	n/a	n/a
Land	ERA5	2003-04 2016-04	0l.45 -0.72	unknown start of utilisation of OLCI data

CDR-1 & CDR-2 surface type	Ref. dataset	Break point (yyyy-mm)	Step size (kg/m^2)	Event
Ice-free Ocean	Merged Microwave	2009-12	-0.10	start of utilisation of F18 data
Global	AIRS	n/a	n/a	n/a
Global	ERA5	2006-11 2016-04	0.12 0.30	start of utilisation of F17 data start of utilisation of OLCI data

Additionally the change of the bias with time, i.e. the temporal stability, is analysed. Figure 5-1 to Figure 5-3 show the time series of the bias relative to AIRS, ERA5 (each land and global) and Merged Microwave (ocean). The figures also include results from linear regression applied to the bias time series (full overlap and time series without OLCI data, i.e. until March 2016) and as vertical lines, break points detected by the homogeneity test. The stability values are given in Table 5-2. Overall the stability estimate is negative over land, i.e., the bias decreases over time, and is positive over ocean, i.e., the bias increases over time. On a global scale the ocean contribution dominates and the overall stability estimate is positive. The positive trend in bias over ocean is affected by a potential break point (see discussion above). Note that Schröder et al. (2016, 2019) showed that trend estimates from REMSS and HOAPS TCWV data agree within uncertainties.

It is noted that a seeming small break point in 2010-12 / 2011-01 is not detected. This seeming break point was discussed above already and is associated with changes in cloud masking differences between MERIS and MODIS and the sampling of the clear-sky bias. Table 5-2 also provides the stability estimate when using ERA5 clear-sky data at 10:00 local time over the period July 2002 – March 2016: 0.02±0.02 kg/m^2/decade. This way the impact from differences in cloud masking is avoided and the stability estimate is at least closer to the true estimate associated with TCWV retrieval.

In summary, when looking at the period July 2002 – March 2016 and at clear-sky data the stability is better than the target requirement, though partly not significantly.

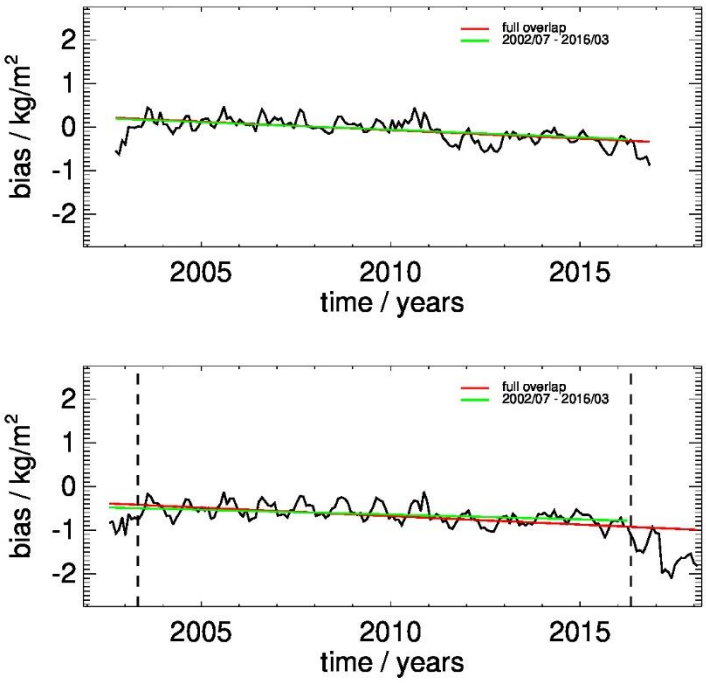

Figure 5-1: Time series of bias between CDR-1 and AIRS (top panel) as well as ERA5 (bottom panel) over global land surfaces. A linear fit is shown for the full overlapping period and the period excluding OLCI data. Dashed vertical lines mark break points detected by the PMF test.

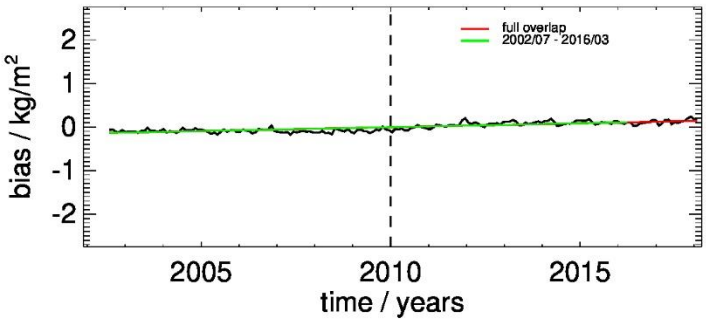

Figure 5-2: As Figure 5-1 but for CDR-2 against Merged Microwave over global ice-free ocean surfaces.

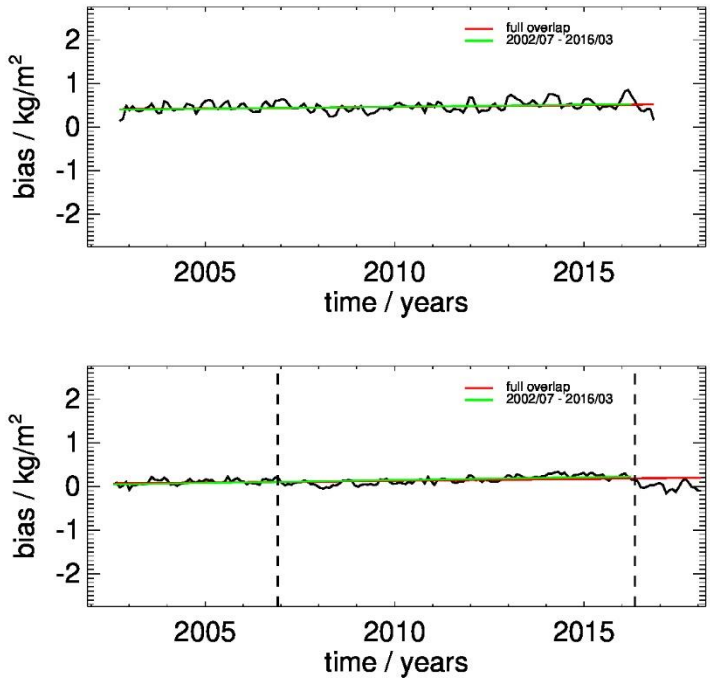

Figure 5-3: As Figure 5-1 but for CDR-2 against AIRS (top panel) and ERA5 (bottom panel) over global surfaces.

Table 5-2: Stability of CDR-1 and CDR-2. The full period covers July 2002 – December 2017. Note that AIRS v6 covers the period September 2002 – September 2016. The recommended period covers July 2002 – March 2016. Marked in green is where the stability is significantly better than the target product requirement of 0.2 kg/m^2/decade (PSD, v3.2, Table 7-2)

CDR-1 & CDR-2 surface type	Ref. dataset	Stability (kg/m^2/decade) (full overlap period)	Stability(kg/m^2/ decade) (recommended period)
Land	AIRS	-0.39±0.09	-0.35±0.09
Land	ERA5	-0.39±0.09	-0.22±0.09
Ice-free Ocean	Merged Microwave	0.18±0.04	0.18±0.05
Global	AIRS	0.08±0.06	0.09±0.08
Global	ERA5	0.09±0.05	0.13±0.05

CDR-1 & CDR-2 surface type	Ref. dataset	Stability (kg/m^2/decade) (full overlap period)	Stability(kg/m^2/decade) (recommended period)
Land	ERA5 clear-sky, 10 LT	-0.11±0.02	0.02±0.02

6. UNCERTAINTY ASSESSMENT

According to the PVP v3.2, the consistency of a CDR and a reference dataset is analysed by comparing the difference of the CDR and the reference to their associated uncertainty estimates (Immler et al., 2010). This is referred to as the “consistency inequality” in Figure 6-1 to Figure 6-3 and Table 7-1. The consistency assessment of uncertainties is assessed considering all valid (daily) collocations on a monthly basis. The expectation is that 68%, 95% and 99% of the cases exhibit validity of the inequality equation for k=1, k=2 and k=3, respectively. If not given this is an indication that the total uncertainty is underestimated or overestimated. While in this section results are plotted as difference as function of total uncertainty results from simple counting of valid cases are provided in Table 7-1.

The unknown in the consistency inequality according to the PVP v3.2 is the representativeness, σ. Because mainly gridded data records are validated the representativeness error is assumed to be small, i.e. σ=0 kg/m^2. When using station-based data instead of gridded data records this assumption may lead to an underestimation of the total uncertainty and to an underestimation of the expectation.

The uncertainty propagation is also explained in the PVP v3.2. Here, it is assumed that the number of hours times the number of days (number of hours) with valid observations gives an estimate of the effective number of independent observations within a month (day). Then, an uncertainty correlation of c=0 is applied. This is the current best estimate of the propagated uncertainty. This approach might not be optimal and impacts the results.

Finally, it needs to be mentioned, that outliers were not filtered and that the PDF of the bias is not perfectly Gaussian. This will affect the consistency assessment as well. Depending on the skewness it can lead to over- and underestimations of the expectation. E.g., long tails of positive and negative biases will lead to a seeming underestimation of total uncertainty.

6.1 Uncertainty assessment in CDR-1

Figure 6-1 and Figure 6-2 summarise the results from consistency analysis between CDR-1 and GRUAN as well as SuomiNet, respectively. It can be seen that in most bins the values stay below the k=1 line and nearly all values are below the k=3 line. Thus, the overall consistency is fairly high, with an overall small overestimation of total uncertainty. When looking closer there seems to be a tendency for underestimating/overestimating the total

uncertainty at values below / above 4.5 kg/m^2 relative to GRUAN and SuomiNet. Relative to the SuomiNet dataset values around 11 kg/m^2 exhibit a strong underestimation. This feature is likely dominated by outliers as observed in Figure 4-12. It is assumed that this is associated with inland water bodies. This is an extreme example of non-Gaussian behaviour impacting the consistency analysis.

When looking at results associated with maximum number of valid data pairs, an underestimation of total uncertainty is observed. This may partly be explained by the assumption that the representativeness error of the station data cannot be neglected. Also, CDR-1 samples TCWV predominantly under clear-sky conditions. This sampling might lead to a clear-sky bias such that the clear-sky data is drier than an all-sky dataset. For monthly data this effect is in the order of approximately 0.9 kg/m^2 or 10% (see CAR v3.0, Sohn and Bennartz, 2008) and is assumed to explain a large part of the difference between monthly and daily comparisons to ERA5 over land (see Figure 4-5). In the consistency analysis over land daily data is considered where this affect is considerably smaller and depends on cloud masking differences between sensors (see Figure 4-5). This may partly explain the seeming underestimation of total uncertainty. Note that the estimation of the strength of the clear-sky bias is valid for monthly data only.

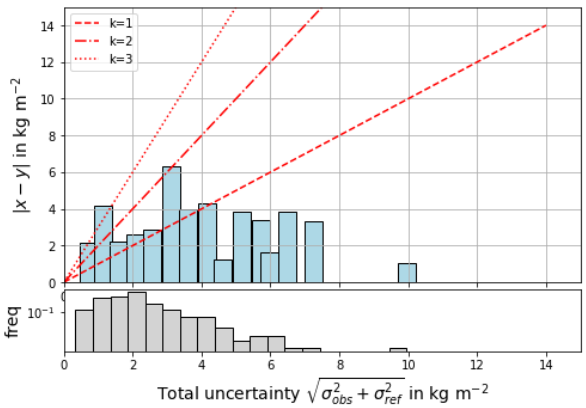

Figure 6-1: Immler inequation plotted for consistency analysis between CDR-1 fv3.1 and GRUAN. The middle of the bar indicates its mean value of the total uncertainty.

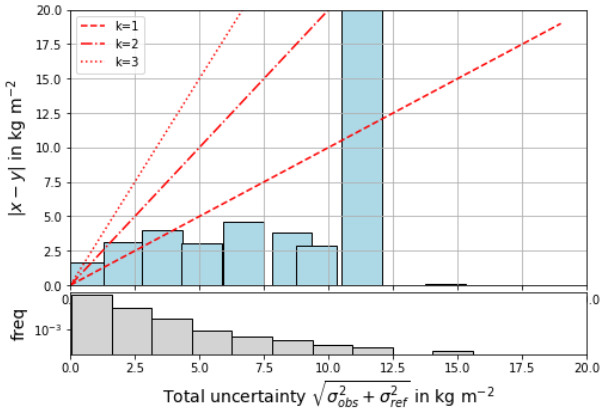

Figure 6-2: Immler inequation plotted for consistency analysis between CDR-1 fv3.1 and SuomiNet. The middle of the bar indicates its mean value of the total uncertainty.

6.2 Uncertainty assessment over ice-free ocean from CDR-2

For the Merged Microwave reference dataset, an uncertainty estimate was extracted from the spread of the Merged Microwave ensemble containing 50 ensemble members. As statistical measure for the spread, the standard deviation was chosen. As the Merged Microwave dataset contains monthly means, the consistency is analysed using all valid monthly collocations.

Figure 6-3 summarises the results from consistency analysis between CDR-2 and Merged Microwave over the global ice-free ocean. It can be seen that in most bins the values stay below the k=1 line and all values are below the k=3 line. This is an indication that the uncertainty is overestimated, except at small total uncertainties. This could have been expected because the retrieval for TCWV using microwave observations is used to simultaneously retrieve TCWV, wind and LWP and thus, includes relaxed uncertainties. Note also the consistency results shown in Table 7-1.

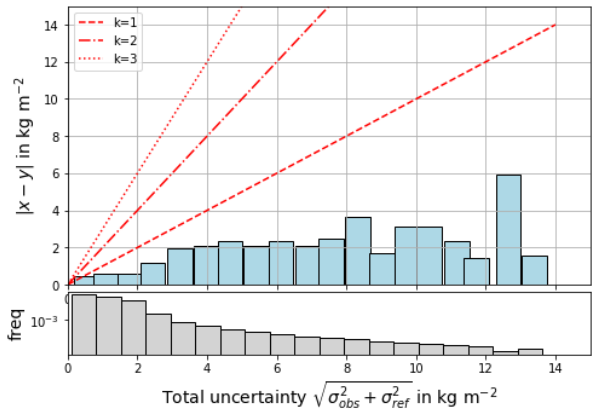

Figure 6-3: Immler inequation plotted for consistency analysis between CDR-2 fv3.1 and Merged Microwave over ice-free ocean. The middle of the bar indicates its mean value of the total uncertainty.

7. OVERALL STATISTICS AND COMPLIANCE WITH REQUIREMENTS

The spatially and temporally averaged mean statistics of the validation and comparison results are shown in Table 7-1 (except stability in Table 5-2). The difference between surface types “global” and “global land and ocean” is that “global” also considers regions over sea-ice and coastal regions.

GOME Evolution provides standard deviation as uncertainty estimate only while ARSA data does not contain any uncertainty estimate. Thus, both are not considered in consistency analysis, i.e. columns following cRMSD are n/a.

Absolute maximum biases are observed between CDR-1 and ARSA (-1.7 kg/m^2) and between CDR-2 over ice-free ocean and AIRS (0.9 kg/m^2). The maximum cRMSD is found between CDR-2 (global) and GOME Evolution: 3.32 kg/m^2. The comparison of CDR-2 over ice-free ocean with Merged Microwave and ERA5 exhibits the smallest bias and minimum cRMSD. It was anticipated that the quality is lower over coastal areas and sea-ice regions. This is reflected in cRMSD being larger in the global analysis than in the global land and ocean analysis.

In the following, the achieved overall accuracies (relative to GRUAN) and disagreements (relative to all other data records) are compared to the product requirements. The product requirements are recalled in Table 7-2. The compliance with target product requirements is generally good for the bias. Exceptions are: CDR-1 vs ERA5, CDR-2 ice-free ocean vs AIRS, and CDR-2 global land and ocean vs GOME Evolution. The cRMSD is always better than the target requirement, except for comparisons to GOME Evolution. It is further assessed if the total sum of uncertainties is larger than the bias-corrected robust standard deviation (PVP v3.2). This is valid in the majority of cases, with the majority of exceptions for CDR-1. However, the consistency being close to the expectation is not met in the majority of cases, with the main exception for CDR-2 over ice-free ocean. The exceptions might be explained by reasons given in the introduction to section 6. Also, the uncertainty for the ERA5 and Merged Microwave datasets are taken from the ensemble spread. It is assumed that the ERA5 uncertainty and the uncertainty for the Merged Microwave product are underestimated. While the underestimation of uncertainties for ERA5 might partly explain the low consistency and the total uncertainty being smaller than RSD_{bias}, both assumed underestimations of uncertainties (ERA5 and Merged Microwave) might give an indirect hint that the uncertainty of CDR-2 over ice-free ocean is actually overestimated. This is actually assumed as the retrieval of TCWV using microwave observations is used to simultaneously retrieve TCWV, wind and LWP and thus, includes relaxed uncertainties.

Finally, the threshold stability requirement is met in all cases while the target requirement is met mainly for CDR-2 global and ice-free ocean. When looking at the period July 2002 – March 2016 and at clear-sky data the stability is better than the target requirement, though partly not significantly (see Table 5-2).

Table 7-1: Summary of statistics and uncertainty assessment for CDR-1 and CDR-2. Marked in green is where the bias estimate is significantly smaller than the target product requirement (PSD, v3.2). Consistency is marked green when it is close to the expected value (arbitrary differences apply). Consistency is not estimated for ARSA and GOME Evolution (see text)

CDR-1 & CDR-2 Land surface	Ref. dataset	Mean bias (kg/m^2)	Mean cRMSD (kg/m^2)	σ_{total} (kg/m^2)	σ_{total} / $TCWV_{mean}$ (%)	RSD_{bias} (kg/m^2)	Consistency (%)		
							k=1	k=2	k=3
Land	ERA5	-0.70±0.37	2.11	0.50	3.5	1.57	31	55	70
Land	AIRS	-0.10±0.27	1.78	0.48	3.4	1.10	81	97	99
Land	SuomiNet	0.10±0.93	2.85	0.73	5.3	2.0	25	50	100
Land	GRUAN	-0.41±1.13	2.52	0.71	6.0	1.72	32	53	71
Land	ARSA	-1.7±1.1	2.44	n/a	n/a	n/a	n/a	n/a	n/a
Land	C3S	-0.10±0.13	1.67	0.55	3.8	0.54	55	83	94
Ice-free Ocean	Merged Microwave	-0.0±0.10	0.69	0.85	3.7	0.43	75	92	97
Ice-free Ocean	AIRS	0.90±0.15	1.16	0.84	3.8	0.75	87	99	100
Ice-free Ocean	ERA5	0.72±0.08	0.63	0.86	3.9	0.63	63	92	97
Ice-free Ocean	C3S	-0.05±0.07	1.50	0.77	3.8	0.54	98	100	100
Global	AIRS	0.47±0.12	1.66	1.14	6.0	0.64	62	69	71
Global	ERA5	0.10±0.10	1.86	1.18	6.2	0.60	50	65	69

CDR-1 & CDR-2 Land surface	Ref. dataset	Mean bias (kg/m^2)	Mean cRMSD (kg/m^2)	σ_{total} (kg/m^2)	σ_{total} / $TCWV_{mean}$ (%)	RSD_{bias} (kg/m^2)	Consistency (%)		
							k=1	k=2	k=3
Global	C3S	-0.05±0.07	1.50	0.77	3.8	0.54	82	94	98
Global	GOME Evl	0.60±0.18	3.32	n/a	n/a	n/a	n/a	n/a	n/a
Global land+ocean	AIRS	0.60±0.11	1.49	0.75	3.9	0.63	85	98	100
Global land+ocean	ERA5	0.23±0.10	1.50	0.76	3.9	0.56	52	80	88
Global land+ocean	C3S	0.06±0.08	1.12	0.77	3.8	0.50	84	95	98
Global land+ocean	GOME Evl	0.75±0.18	3.24	n/a	n/a	n/a	n/a	n/a	n/a

Table 7-2: Overview of CDR-1 and CDR-2 product requirements. The WV_cci product requirements are given as target requirements (see also PSD v3.2). As CDR-2 is released via EUMETSAT CM SAF, CM SAF threshold and optimum requirements are also given, with the target requirements being identical to the WV_cci product requirements

Metric	Threshold	Target	Optimum
Accuracy (systematic component) (kg/m^2)	3.0	1.0	0.3
Precision (random component) (kg/m^2)	5.0	3.0	0.3
Stability (kg/m^2/decade)	0.70	0.20	0.08

The user requirements (URD v3.0) for systematic and random components of the accuracy are 25%, 5% and <1% for threshold, target and optimum, respectively. GCOS requirements on measurement uncertainty and stability are 2% and 0.3 % per decade, respectively

(GCOS, 2016), When computing the relative bias using the mean TCWV from CDR-2 (~19 kg/m^2) the maximum absolute relative bias is 8.9% between CDR-1 and ARSA. All other relative biases are better than the target user requirement. A bias of 0.38 kg/m^2 would translate into a relative bias of 2% and thus, in nine cases the relative bias is smaller than the GCOS requirement. The latter is in particular true for comparisons between CDR-1 and AIRS as well as SuomiNet, between CDR-2 ocean and Merged Microwave and between CDR-2 and ERA5. As the total uncertainty contains the uncertainty from reference and CDR it can be concluded from Table 7-1 that CDR-1 and CDR-2 exhibit requirements close to the target user requirement of the random component of the uncertainty (for orientation – the maximum relative total uncertainty is 6.2%). A relative total uncertainty being smaller than the GCOS requirement of 2% is not observed. Note however that the expectation from the Immler inequation is not met in all cases. Finally when transferring the stability values into relative values using the mean TCWV from CDR-2 the maximum relative stability is 2.1% per decade (CDR-1 vs ERA5). Thus, all values are within threshold stability user requirement. Values < 0.18 kg/m^2/decade translate into values better than the target user requirement of 1% per decade. The GCOS requirement on stability is met only between CDR-1 and the ERA5 clear-sky, 10 LT version.

8. SUMMARY

This Product Validation and Intercomparison Report (Part 1) describes the quality of the WV_cci data records CDR-1 and CDR-2. Both consist of TCWV in unit kg/m^2, cover the period July 2002 – December 2017, and the former covers land areas while the latter is a global product. The PVIR is based on a wide range of reference and comparison data records, various approaches to assess the quality of the product including consistency analysis using uncertainties and assess the compliance with requirements. Future efforts would benefit from information on uncertainty correlations c and on the representativity error. In the future impact studies assuming specific c and represemtativity errors and further assuming that the clear-sky bias can on average be applied to daily data can be carried out to at least describe their potential effect on the propagated uncertainty and consistency. The focus in this PVIR is on analysing results from comparisons to various satellite, reanalysis, ground-based and *in situ* data records. It was demonstrated that CDR-1 and CDR-2 are well within threshold product requirements and frequently meet the target product requirement and user requirements. It is noted that the quality over inland water bodies, coastal areas and sea-ice is lower. Depending on the user application, it might be prudent to filter the data accordingly. It was also observed that the transition between MODIS and OLCI based TCWV over land is associated with a break point and should thus be excluded from climate change analysis. The NIR based TCWV data over land exhibits a high stability when OLCI data is removed and only clear-sky data is considered. Over ocean a small break point was observed. However, the stability is still better than the target product requirement, though not significantly.

APPENDIX 1: REFERENCES

ATBD (2021) Algorithm Theoretical Basis Document, Part 1 - MERIS-MODIS-OLCI L2 Products. ESA/ECSAT, WV_cci Phase One, Ref: CCIWV.REP.004, version 2.1, 21 January 2021.

Calbet, X., Peinado-Galan, N., Rípodas, P., Trent, T., Dirksen, R., and Sommer, M.: Consistency between GRUAN sondes, LBLRTM and IASI, Atmos. Meas. Tech., 10, 2323–2335, https://doi.org/10.5194/amt-10-2323-2017, 2017.

CAR (2021) Climate Assessment Report. ESA/ECSAT, WV_cci Phase One, Ref: CCIWV.REP.018, v2.0, in progress.

DARD (2021) Data Access Requirement Document. ESA/ECSAT, WV_cci Phase One, Ref: CCIWV.REP.003, version 3.2, 27 July 2021.

GCOS, The Global Climate Observing System for Climate: Implementation Plan. WMO GCOS-200, 341 pp., 2016. Available at https://library.wmo.int/doc_num.php?explnum_id=3417 [accessed 15 January, 2021].

Ghent, D., Veal, K., Trent, T., Dodd, E., Sembhi, H. and Remedios, J., 2019. A new approach to defining uncertainties for MODIS land surface temperature. Remote Sensing, 11(9), p.1021.

Hegglin, M. I., et al. (2013), SPARC Data Initiative: Comparison of water vapor climatologies from international satellite limb sounders, J. Geophys. Res. Atmos., 118, 11,824–11,846, doi:10.1002/jgrd.50752.

Iglewicz, B. and Hoaglin, D.C., 1993. How to detect and handle outliers (Vol. 16). Asq Press.

Immler, F., Dykema, J., Gardiner, T., Whiteman, D., Thorne, P., & Vömel, H. (2010). Reference quality upper-air measurements: Guidance for developing GRUAN data products. Atmospheric Measurement Techniques, 3(5), 1217–1231

Mears, C. A., Smith, D. K., Ricciardulli, L., Wang, J., Huelsing, H., & Wentz, F. J. (2018). Construction and uncertainty estimation of a satellite-derived total precipitable water data record over the world's oceans. Earth and Space Science, 5(5), 197-210.

PVASR (2021) Product Validation and Selection Report, ESA/ECSAT, WV_cci Phase One, Ref: CCIWV.REP.009, version 2.2, 17 August 2021.

Reeves, J., Chen, J., Wang, X.L., Lund, R. and Lu, Q. (2007): A review and comparison of changepoint detection techniques for climate data. J. Appl. Meteorol. Climatol., 46, 900–915.

PSD (2021) Product Specification Document. ESA/ECSAT, WV_cci Phase One, Ref: CCIWV.REP.008, version 3.2, 27 July 2021.

PVP (2021) Product Validation Plan. ESA/ECSAT, WV_cci Phase One, Ref: CCIWV.REP.002, version 3.2, 29 July 2021.

Schröder, M., M. Lockhoff, J. Forsythe, H. Cronk, T. H. Vonder Haar, R. Bennartz, 2016: The GEWEX water vapor assessment (G-VAP) – results from the trend and homogeneity analysis. J. Applied Meteor. Clim., 1633-1649, 55 (7), https://dx.doi.org/10.1175/JAMC-D-15-0304.1.

Schröder, M., M. Lockhoff, L. Shi, T. August, R. Bennartz, H. Brogniez, X. Calbet, F. Fell, J. Forsythe, A. Gambacorta, S.-P. Ho, E. R. Kursinski, A. Reale, T. Trent, Q. Yang, 2019: The GEWEX

water vapor assessment of global water vapour and temperature data records from satellites and reanalyses. Rem. Sens., 11(3), 251, https://doi.org/10.3390/rs11030251.

Sohn, B. J., & Bennartz, R., 2008: Contribution of water vapor to observational estimates of longwave cloud radiative forcing. *Journal of Geophysical Research: Atmospheres*, *113*(D20).

SPARC, 2017: The SPARC Data Initiative: Assessment of stratospheric trace gas and aerosol climatologies from satellite limb sounders. By M. I. Hegglin and S. Tegtmeier (eds.), SPARC Report No. 8, WCRP-5/2017, doi:10.3929/ethza-010863911. (available at www.sparc-climate.org/publications/sparc-reports/sparc-reportno8/).

URD (2021) User Requirement Document, ESA/ECSAT, WV_cci Phase One, Ref: CCIWV.REP.001, version 3.0, 11 February 2021.

Wang, X.L. (2008a): Penalized maximal F test for detecting undocumented mean shift without trend change. J. Atmos. Ocean. Technol. 25, 368–384.

Wang, X.L. (2008b): Accounting for autocorrelation in detecting mean shifts in climate data series using the penalized maximal t or F test. J. App. Meteor. Climatol. 47, 2423–2444.

APPENDIX 2: GLOSSARY

Term	Definition
ABC(t)	Atmosphere Biosphere Climate (teledetection)
ACE-FTS	Atmospheric Chemistry Experiment Fourier Transform Spectrometer
ACE-MAESTRO	Atmospheric Chemistry Experiment Measurements of Aerosol Extinction in the Stratosphere and Troposphere Retrieved by Occultation
AMSR-E	Advanced Microwave Scanning Radiometer for EOS
AMSU	Advanced Microwave Sounding Unit
ARA	Atmospheric Radiation Analysis
ARSA	Analyzed RadioSoundings Archive
AVHRR	Advanced Very High Resolution Radiometer
BC	Brockmann Consult
CARIBIC	Civil Aircraft for the Regular Investigation of the atmosphere Based on an Instrument Container
CCI	Climate Change Initiative
CDO	Climate Data Operators
CDR	Climate Data Record
CDS	Copernicus Climate Data Store
CEDA	Centre for Environmental Data Analysis
CF	Conventions for Climate and Forecast
CM SAF	EUMETSAT Satellite Application Facility on Climate Monitoring
CMAM	Canadian Middle Atmosphere Model
CMIP	Coupled Model intercomparison Project
CMUG	Climate Modelling User Group
CRG	Climate Research Group
DLR	Deutschen Zentrums für Luft- und Raumfahrt
DWD	Deutscher Wetterdienst (German MetService)
ECCC	Environment and Climate Change Canada
ECMWF	European Centre for Medium-Range Weather Forecasts
ECV	Essential Climate Variable
EDA	ERA5 - reduced resolution ten member ensemble
EMiR	ERS/Envisat MWR Recalibration and Water Vapour Thematic Data Record Generation
Envisat	Environmental Satellite

Term	Definition
ERA5	ECMWF Re-Analysis 5
ERA-Interim	ECMWF Re-Analysis Interim
ESA	European Space Agency
EUMETSAT	European Organisation for the Exploitation of Meteorological Satellites
FOV	Field of View
FPH	Frost Point Hygrometer
GCOS	Global Climate Observing System
GEOS-5	Goddard Earth Observing System Model, Version 5
GMI	Global Precipitation Microwave Imager
GNSS	Global Navigation Satellite System
GOMOS	Global Ozone Monitoring by Occultation of Stars
GOZCARDS	Global OZone Chemistry And Related trace gas Data records for the Stratosphere
GPS	Global Positioning System
GRUAN	GCOS Reference Upper-Air Network
GUM	Guide to the Expression of Uncertainty in Measurement
HARMOZ	HARMonized dataset of Ozone profiles
HALOE	Halogen Occultation Experiment
HIRDLS	High Resolution Dynamics Limb Sounder
HOAPS	Hamburg Ocean Atmosphere Parameters and Fluxes from Satellite Data
IAGOS	In-service Aircraft for a Global Observing System
IASI	Infrared Atmospheric Sounder Interferometer
ILAS-II	Improved Limb Atmospheric Spectrometer-II
IMS	Infrared Microwave Sounding
IPSL-CM	Institut Pierre Simon Laplace Climate Model
IR	Infrared
LMD	Laboratoire Météorologie Dynamique
LMS	Lowermost stratosphere
LST	Land Surface Temperature
LWP	Vertically integrated liquid water
MERIS	Medium Resolution Imaging Spectrometer Instrument
MERRA-2	Modern-Era Retrospective analysis for Research and Applications, Version 2
MHS	Microwave Humidity Sounder

Term	Definition
MIPAS	Michelson Interferometer for Passive Atmospheric Sounding
MLS	Microwave Limb Sounder
MODIS	Moderate Resolution Imaging Spectrometer
MOZAIC	Measurement of OZone by Airbus In-service airCraft
MPI-M	Max-Planck Institute for Meteorology
MUDB	Match-up database
NASA	National Aeronautics and Space Administration
NCAR	National Center for Atmospheric Research
NCEO	National Centre for Earth Observation
NCEP	National Centers for Atmospheric Prediction
NDVI	Normalized Difference Vegetation Index
NIR	Near IR
NOAA	National Oceanic & Atmospheric Administration
NWP	Numerical Weather Prediction
OLCI	Ocean and Land Colour Instrument
PCs	Principle components
POAM	Polar Ozone and Aerosol Measurement
PSD	Product Specification Document
RAL	Rutherford Appleton Laboratory
RMS	Root mean square
RR	Reduced resolution
RTTOV	Radiative Transfer for TOVS
SAGE	Stratospheric Aerosol and Gas Experiment
SASBE	Site Atmospheric State Best Estimate
SCIAMACHY	Scanning Imaging Absorption Spectrometer for Atmospheric Cartography
SCISAT	Scientific Satellite
SE	Spectral Earth
SMILES	Solar wind Magnetosphere Ionosphere Link Explorer
SMR	Software Modification Report
SNR	Signal-to-noise ratio
SOFIE	Solar Occultation For Ice Experiment
SPARC	Stratosphere-troposphere Processes And their Role in Climate

Term	Definition
SPURT	Spurenstofftransport in der Tropopausenregion, trace gas transport in the tropopause region
SSM/I	Special Sensor Microwave Imager
SSMIS	Special Sensor Microwave Imager Sounder
SST	Sea Surface Temperature
SuomiNet	Global ground based GPS network (named after Verner Suomi)
SWOOSH	Stratospheric Water and OzOne Satellite Homogenized data set
TBD	To be determined
TCWV	Total Column Water Vapour
TMI	Tropical Rainfall Measuring Mission's Microwave Imager
TOA	Top Of Atmosphere
UKMO	United Kingdom Meteorological Office
UoL	University of Leicester
UoR	University of Reading
URD	User Requirements Document
UT	Upper Troposphere
UTLS	Upper Troposphere and Lower Stratosphere
UV	Ultraviolet
vis	Visible
VMR	Volume mixing ratio
VRes	Vertically resolved
WACCM	Whole Atmosphere Community Climate Model
WAVAS-I	Water Vapour Assessment
WAVAS-II	Water Vapour Assessment 2
WCRP	World Climate Research Programme
WGS	World Geodetic System 1984
WMO	World Meteorological Organization
WV	Water Vapour
WV_cci	Water Vapour climate change initiative

APPENDIX 3: SUOMINET TEMPORAL COVERAGE

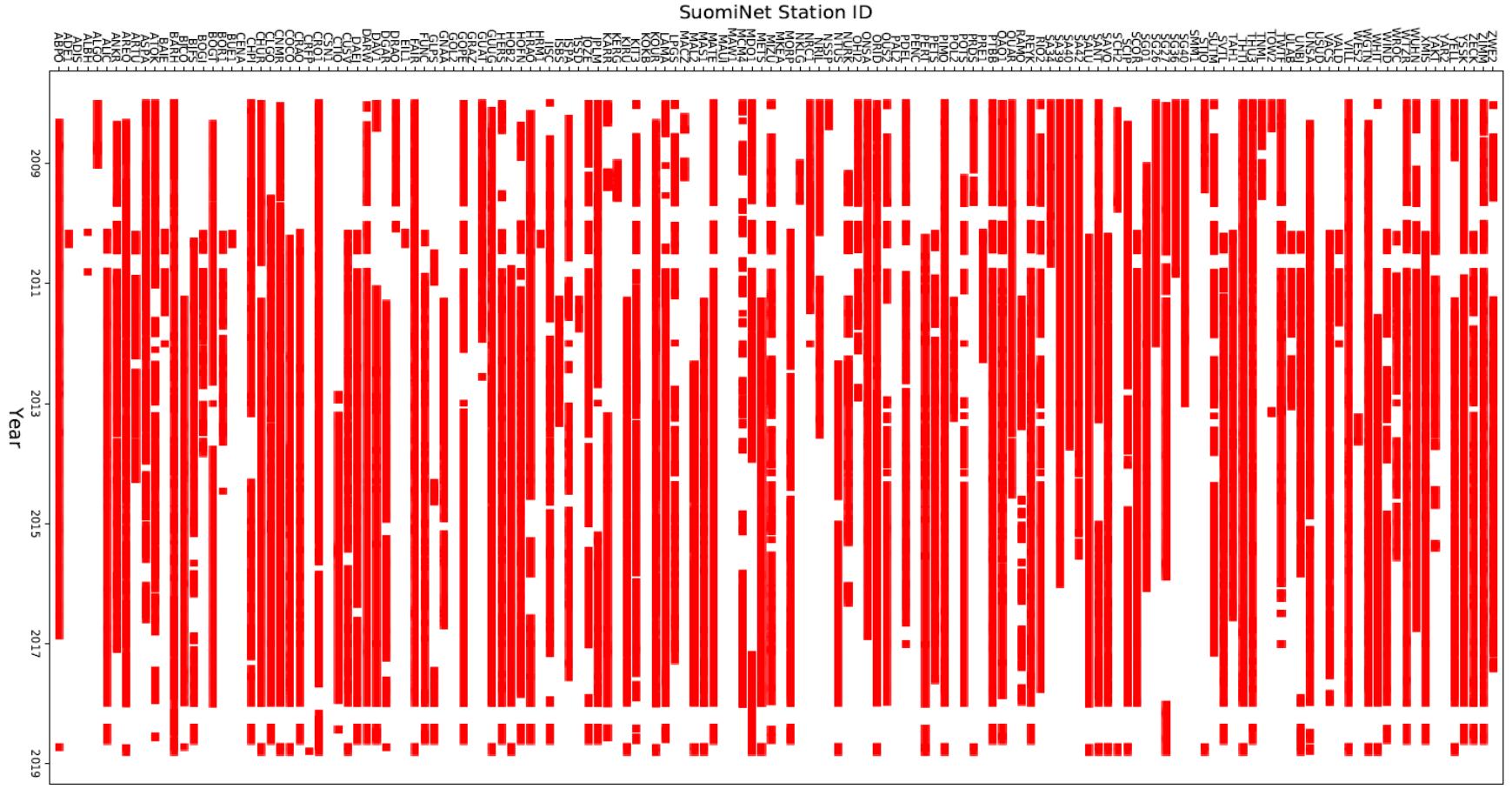

Figure A3-0-1: Temporal coverage of TCWV data records at each SuomiNet GPS station between 2008 and 2018 based on GPS files downloaded from https://www.suominet.ucar.edu/data/ncGlobalDaily

End of Document